

Vacuum Ultraviolet Generation via Wave-Mixing

Nonlinear medium

- crystals
- metal vapors
- noble gases

Again Maxwell's framework:
coupled wave equations

$$\frac{d}{dz} \mathbf{E}_q = i \frac{2\pi(q\omega)^2}{ck_q} \mathbf{P}_q^{NL}$$

\mathbf{E}_q and \mathbf{P}_q^{NL}

Fourier components of fields at
frequency $q\omega$
Fields:

$$\mathbf{E}_q = \hat{\mathbf{E}}_q(z, t) \exp[ik_q z]$$

Nonlinear polarization has several terms:

$$\mathbf{P}_3^{NL} = \frac{N}{4} \left[\underline{3\chi_T^{(3)}(3\omega)\mathbf{E}_1\mathbf{E}_1\mathbf{E}_1} + \chi_S^{(3)}(3\omega)\mathbf{E}_3|\mathbf{E}_3|^2 + \chi_S^{(3)}(\omega, 3\omega)\mathbf{E}_3|\mathbf{E}_1|^2 \right]$$

THG

General issues in

four wave mixing or third harmonic generation:

Susceptibility of the medium :

involves transition dipoles in atoms and resonances

Transparency : problems at short wavelengths

Phase-matching :

including the effects of focused laser beams

Practical limitation: optical breakdown

Phase-matching and focusing

Three processes of four-wave mixing:

I $\omega_1 + \omega_2 + \omega_3 \rightarrow \omega_4$

II $\omega_1 + \omega_2 - \omega_3 \rightarrow \omega_4$

III $\omega_1 - \omega_2 - \omega_3 \rightarrow \omega_4$

Electric fields:

$$\mathbf{E}(\mathbf{r}, t) = \text{Re}[\mathbf{E}_1(\mathbf{r})\exp(-i\omega_1 t) + \mathbf{E}_2(\mathbf{r})\exp(-i\omega_2 t) + \mathbf{E}_3(\mathbf{r})\exp(-i\omega_3 t)]$$

Define optical beams as lowest order Gaussians for each frequency ω

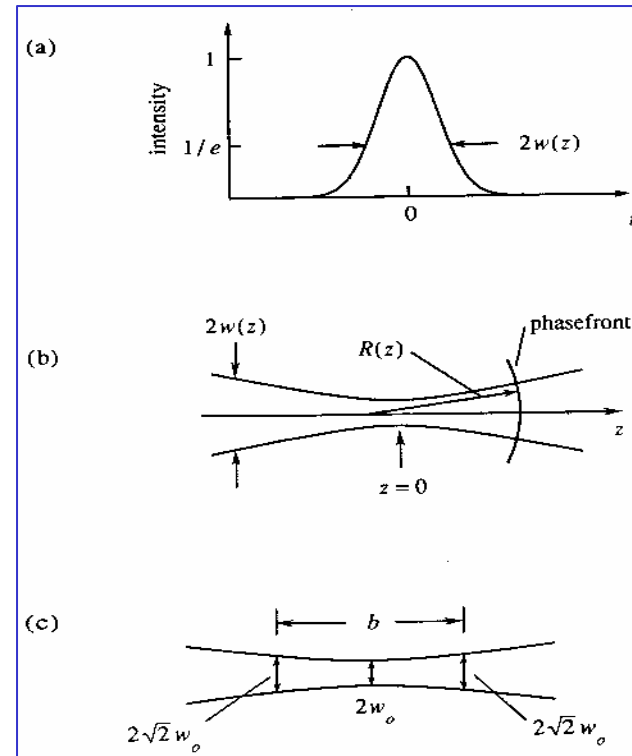
Gaussian beam TM_{00}

(\rightarrow higher order modes give differing results !)

$$\mathbf{E}_n(\mathbf{r}) = \mathbf{E}_{n0}(\mathbf{r}) \frac{\exp(ik_n z)}{1 + i\xi} \exp\left[\frac{-k_n(x^2 + y^2)}{b(1 + i\xi)}\right]$$

Confocal parameter b

$$b = \frac{2\pi w_0^2}{\lambda} = \frac{2\pi w_0^2 n}{\lambda_0} = \frac{2\lambda_0}{n\theta^2} = kw_0^2$$



w_0 beam waist radius

n index of refraction

θ far-field diffraction angle

$$\xi = \frac{2(z - f)}{b} \quad \text{normalized coordinate along } z$$

Nonlinear Polarization

Newly generated field via processes I, II, III

$$P_4(\mathbf{r}) = \frac{3}{2} N \chi^{(3)}(-\omega_4; \omega_1, \omega_2, \omega_3) E_1(\mathbf{r}) E_2(\mathbf{r}) E_3(\mathbf{r})$$

$$P_4(\mathbf{r}) = \frac{3}{2} N \chi^{(3)}(-\omega_4; \omega_1, \omega_2, -\omega_3) E_1(\mathbf{r}) E_2(\mathbf{r}) E_3^*(\mathbf{r})$$

$$P_4(\mathbf{r}) = \frac{3}{2} N \chi^{(3)}(-\omega_4; \omega_1, -\omega_2, -\omega_3) E_1(\mathbf{r}) E_2^*(\mathbf{r}) E_3^*(\mathbf{r})$$

χ the polarizability (per atom) and
 N density of medium
 Note degeneracy factors (field amplitudes);
 those may differ for degenerate fields.

Insert fields with their mode structure:

$$P_4(\mathbf{r}) = \frac{3}{2} N \chi^{(3)}(-\omega_4; \omega_1, \omega_2, \omega_3) E_{10} E_{20} E_{30} \frac{\exp(ik'z)}{(1+i\xi)^3} \exp\left[\frac{-k'(x^2+y^2)}{b(1+i\xi^2)}\right] \quad k' = k_1 + k_2 + k_3 = k'' \quad \text{Process I}$$

$$P_4(\mathbf{r}) = \frac{3}{2} N \chi^{(3)}(-\omega_4; \omega_1, \omega_2, -\omega_3) E_{10} E_{20} E_{30} \frac{\exp(ik'z)}{(1+i\xi)^2(1-i\xi)} \exp\left[\frac{(-k''+i\xi k')(x^2+y^2)}{b(1+\xi^2)}\right] \quad k' = k_1 + k_2 - k_3 \quad \text{Process II}$$

$$P_4(\mathbf{r}) = \frac{3}{2} N \chi^{(3)}(-\omega_4; \omega_1, -\omega_2, -\omega_3) E_{10} E_{20} E_{30} \frac{\exp(ik'z)}{(1+i\xi)(1-i\xi)^2} \exp\left[\frac{(-k''+i\xi k')(x^2+y^2)}{b(1+\xi^2)}\right] \quad k' = k_1 - k_2 - k_3 \quad \text{Process III}$$

Further steps; Maxwell's equations

Derive amplitudes in a Fourier decomposition;
amplitude with wave vector \mathbf{K}

$$P_4(\mathbf{K}) = (2\pi)^{-3} \int_{-\infty}^{\infty} dx'' \int_{-\infty}^{\infty} dy'' \int_{-\infty}^{\infty} dz'' P_4(\mathbf{r}'') \exp[-i\mathbf{K} \cdot \mathbf{r}'']$$

Insert in Maxwell's equation:

$$\nabla \times \nabla \times E_4(\mathbf{K})(\mathbf{r}) - \underbrace{k_4^2}_{\text{medium}} E_4(\mathbf{K})(\mathbf{r}) = 4\pi k_0^2 \underbrace{P_4(\mathbf{K})}_{\text{vacuum}} \exp[i\mathbf{K} \cdot \mathbf{r}]$$

For: $\Delta k = k_4 - k'$

Solutions, process I (similar equations for II and III)

$$E_4(\mathbf{r}) = i \frac{3N}{2k_4} \pi k_0^2 b \chi^{(3)}(-\omega_4; \omega_1, \omega_2, \omega_3) E_{10} E_{20} E_{30} \frac{\exp(ik'z)}{(1+i\xi)} \exp\left[\frac{-k'(x^2+y^2)}{b(1+i\xi)}\right] \int_{-\zeta}^{\xi} \frac{\exp[-(ib/2)\Delta k(\xi'-\xi)]}{(1+i\xi')^2} d\xi'$$

With integration boundaries:

$$\zeta = 2f/b \quad \xi = \frac{2(z-f)}{b}$$

Field $E_4(\mathbf{r})$ to be calculated, integration over x and y , and z to $z=L$.

$$\int_0^{\infty} 2\pi R |E_4(R)|^2 dR \quad R = \sqrt{x^2 + y^2}$$



Result, generally:

- Modes cylindrically symmetric around z -axis
- Only for Process I the generated beam has lowest order Gaussian

The phase-matching can be quantified:

Phase-matching in $\chi^{(3)}$ Processes

Define the phase-matching integrals:

$$F_j\left(b\Delta k, \frac{b}{L}, \frac{f}{L}, \frac{k''}{k'}\right) = \frac{8}{9} \frac{k_4^2 k'}{\pi^3 k_0^4 b^3 \chi^2 |E_{10} E_{20} E_{30}|^2} \int_0^\infty 2\pi R |E_4(R)|^2 dR$$

For all three processes, $j=I, II, III$

Dimensionless parameters, defining geometry and phases.

Then generated Power at P_4 is

$$P_4 = \eta \frac{k_0^4 k_1 k_2 k_3}{k_4^2 k'} N^2 \chi^2 P_1 P_2 P_3 F_j\left(b\Delta k, \frac{b}{L}, \frac{f}{L}, \frac{k''}{k'}\right)$$

Degeneracy factor

Phase-matching integral for Process I

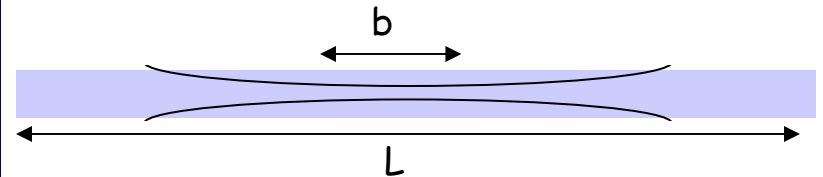
$$F_I\left(b\Delta k, \frac{b}{L}, \frac{f}{L}, \frac{k''}{k'}\right) = \left| \int_{-\zeta}^{\xi} \frac{\exp[-(ib/2)\Delta k \xi']}{(1+i\xi')^2} d\xi' \right|$$

This integral can be evaluated for various conditions, for example in the "tight-focusing limit", $b \ll L$ and integrating

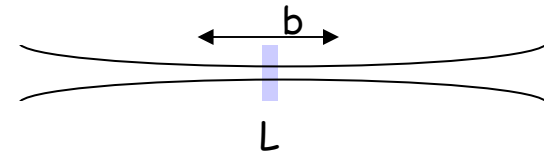
$$\xi \rightarrow \infty \quad \zeta \rightarrow \infty$$

Define:

Tight-focus



Plane wave limit



Phase-matching integrals F_j for processes and geometries

For "tight-focus" $b/L \ll 1$
 "half-way" the cell $f/L = 0.5$

Process I:

$$F_I(b\Delta k, 0, 0.5, 1) = \begin{cases} \pi^2 (b\Delta k)^2 e^{(b\Delta k/2)} & \text{--- } \Delta k < 0 \\ 0 & \text{--- } \Delta k \geq 0 \end{cases}$$

Similarly for Process II and III
 (if $k' = k''$ assumed; lowest order mode)

$$F_{II}(b\Delta k, 0, 0.5, 1) = \pi^2 e^{-b|\Delta k|}$$

$$F_{III}(b\Delta k, 0, 0.5, 1) = \begin{cases} 0 & \text{--- } \Delta k < 0 \\ \pi^2 (b\Delta k)^2 e^{(b\Delta k/2)} & \text{--- } \Delta k \geq 0 \end{cases}$$

General conclusion:

THG (Process I) only possible,
 in the tight-focusing limit if $\Delta k < 0$

So: only if the medium has
NEGATIVE DISPERSION !!

This also holds for sum-frequency mixing

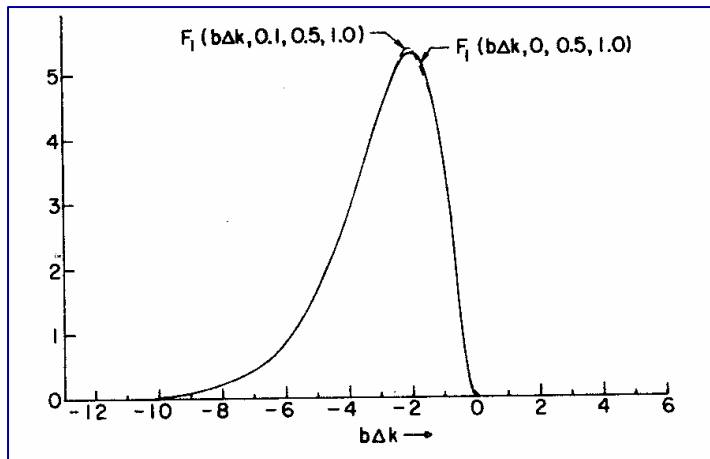
Difference frequency mixing for any k

Numerical approach evaluating F_j ; all near tight focus

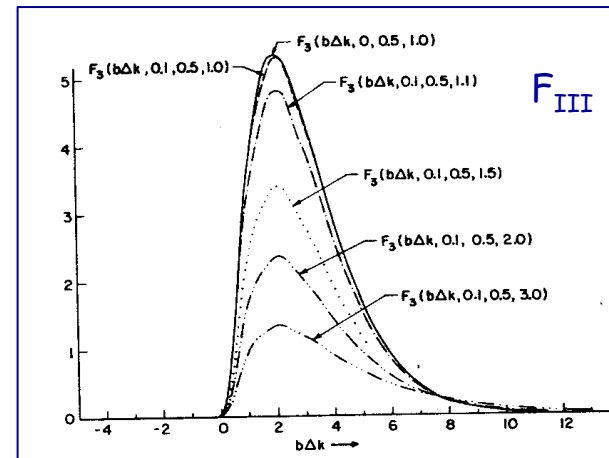
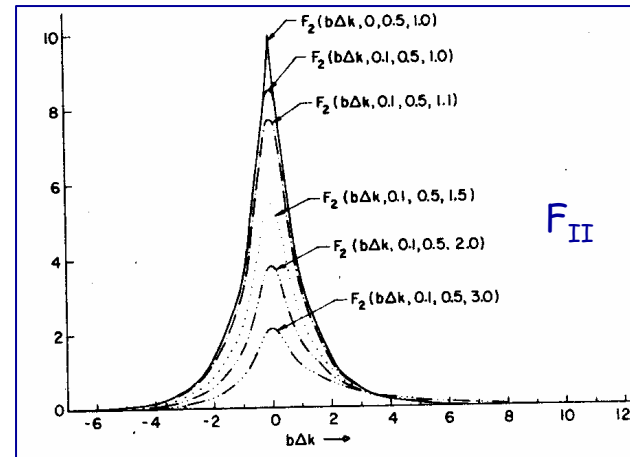
Phase-matching integral including

- 1) Dispersion
- 2) Phase evolution through focal region

$$F_j \left(b\Delta k, \frac{b}{L}, \frac{f}{L}, \frac{k''}{k'} \right)$$

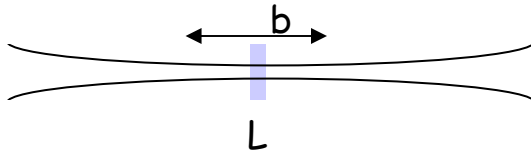


F_I versus $b\Delta k$ for $b/L < 0.1$ and $f/L=0.5$



Varying the tightness of focus b/L and the mode function k''/k'

Results in the "plane-wave" limit



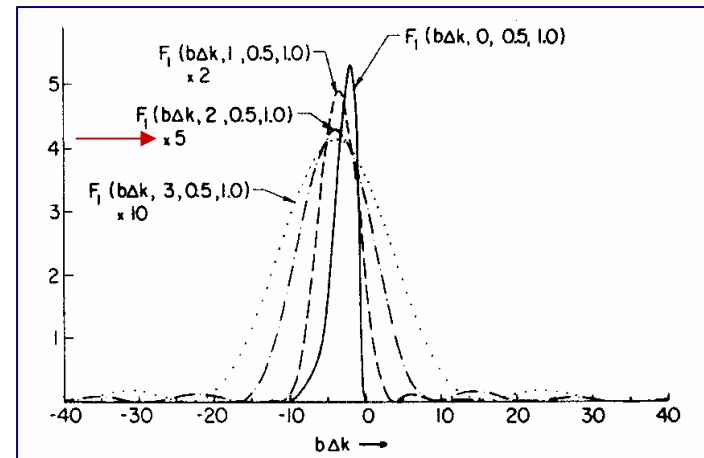
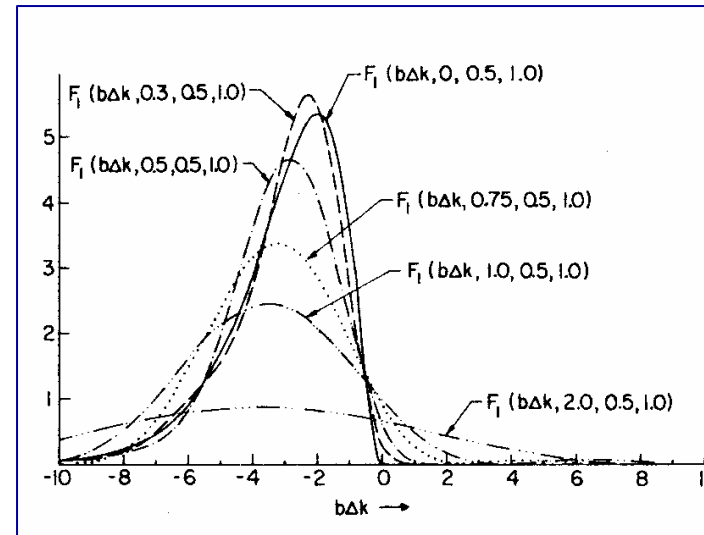
$$\lim_{b/L \rightarrow \infty} F_I \left(b\Delta k, \frac{b}{L}, 0.5, \frac{k''}{k'} \right) = \frac{4L^2}{b^2} \text{sinc}^2 \left(\frac{\Delta k L}{2} \right)$$

Note the similarity with analysis of frequency-doubling in crystal; This was done for plane parallel fields!

At $b/L \sim 3$ the peak has shifted to the real plane-wave limit already, peaking at $\Delta k=0$.

Note also the decrease in intensity for the plane-wave limit case.

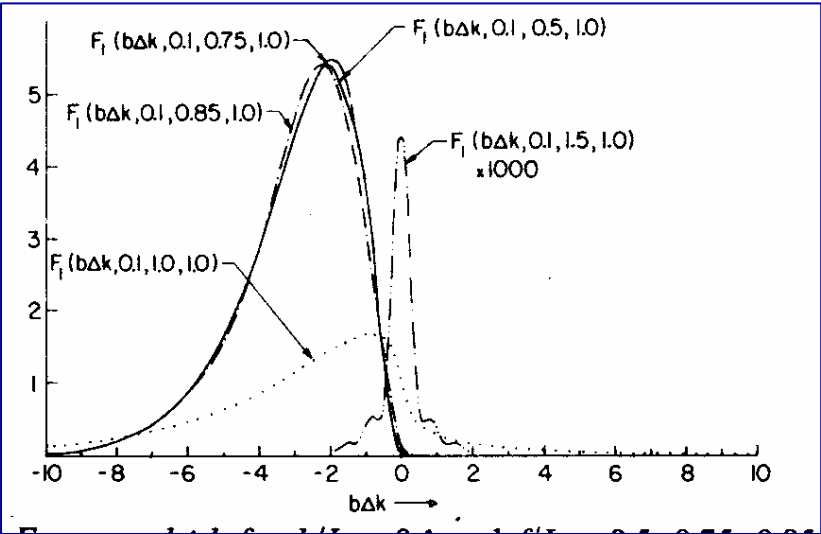
Tight-focusing is more efficient!



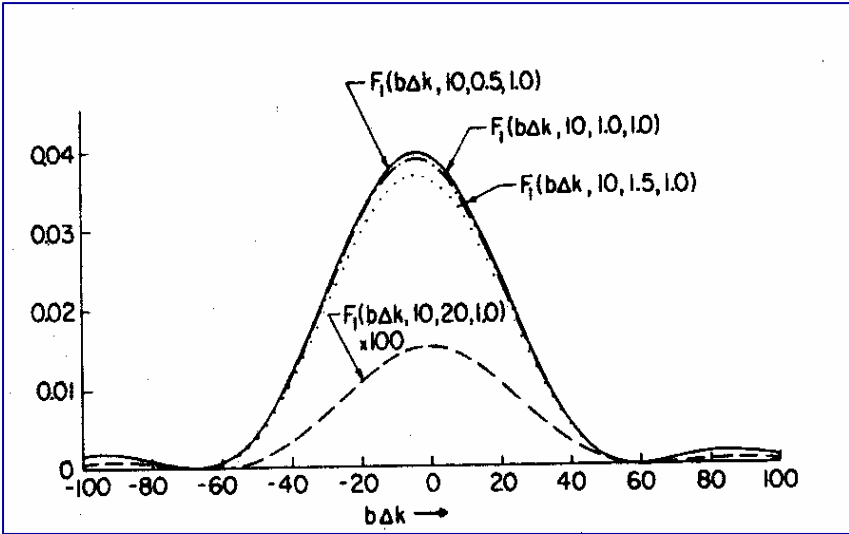
Shifting the focus; playing with the phase build-up

$$F_j \left(b\Delta k, \frac{b}{L}, \frac{f}{L}, \frac{k''}{k'} \right)$$

For near-tight-focusing of $b/L=0.1$
 Focal positions $f/L=0.5$ toward $f/L=1.5$
 In latter case focus shifts outside the cell
 And effectively plane-wave limit is reached.



Near the true plane-wave limit at $b/L=10$
 Only small changes to F-integral as long as
 focus is inside the cell.
 At $f/L=20$ the focus is twice the distance
 of the confocal parameter $b/L=10$.



Physical interpretation of phase-matching integrals

1) Non-linear polarization peaks at the region of the beam WAIST
 → intensity is highest in focus

2) Phase-matching relates to phase-overlap of all beams involved
 For a Gaussian beam:

$$\mathbf{E}_n(\mathbf{r}) = \mathbf{E}_{n0}(\mathbf{r}) \frac{\exp(ik_n z)}{1+i\xi} \exp\left[\frac{-k_n(x^2+y^2)}{b(1+i\xi)}\right]$$

$$\frac{1}{1+i\xi} = \frac{1}{\sqrt{1+\xi^2}} e^{-i \arctan \xi}$$

For tight-focusing:

$$\xi = -2 \quad \longrightarrow \quad z = f - b$$

$$\xi = 2 \quad \longrightarrow \quad z = f + b$$

Boundaries of focus at windows.

Lowest order Gaussian beam undergoes phase shift

$$\arctan \xi$$

when propagating through the focus (Gouy phase), adding up to π for $(-\infty, \infty)$

Driving polarization undergoes

| | |
|-----------------|-------------|
| $3 \arctan \xi$ | Process I |
| $\arctan \xi$ | Process II |
| $-\arctan \xi$ | Process III |

Optimum conversion if generated field is in phase with driving fields.

Generated beam undergoes phase slip: $\arctan \xi$

In-phase for Process II, destructive for I and III

Phase-slips compensated by DISPERSION

| | |
|----------|-----|
| $-2.2/b$ | I |
| 0 | II |
| $2.2/b$ | III |

Optimizing density - dispersion and phase-matching

Nonlinear generation:

$$P_4 \propto P_1 P_2 P_3 N^2 \chi^2 F_j \left(b\Delta k, \frac{b}{L}, \frac{f}{L}, \frac{k''}{k'} \right)$$

$N^2 F_j$ can be optimized by varying
 $N, b\Delta k, b/L, f/L$

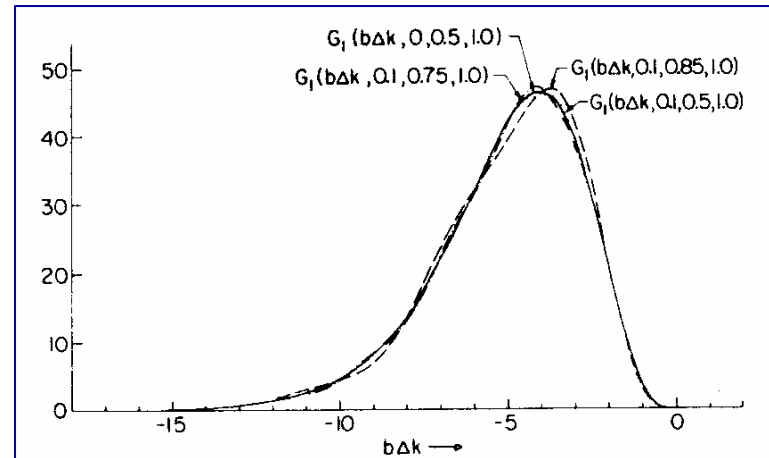
if N varies - macroscopic effect on medium
 - index of refraction changes
 - Δk varies

Phase-mismatch is a dispersion effect and

$$\Delta k = \alpha N$$

One can define a dimensionless quantity:

$$G_j \left(b\Delta k, \frac{b}{L}, \frac{f}{L}, \frac{k''}{k'} \right) = (b\Delta k)^2 F_j \left(b\Delta k, \frac{b}{L}, \frac{f}{L}, \frac{k''}{k'} \right)$$



G_I vs. $b\Delta k$ for tight-focusing; always OK as long as focus inside the cell.

THG production and dispersion in the noble gases

Third harmonic produced:

$$P_{THG} = \frac{\eta}{(3\lambda)^4} N^2 \left[\chi^{(3)}(\lambda) \right]^2 P_1^3 F_j \left(b\Delta k, \frac{b}{L}, 0.5, 1 \right)$$

In tight-focusing limit ($b \ll L$):

$$F_I(b\Delta k, 0, 0.5, 1) = \begin{cases} \pi^2 (b\Delta k)^2 e^{(b\Delta k/2)} & \Delta k < 0 \\ 0 & \Delta k \geq 0 \end{cases}$$

In plane-wave limit ($b \gg L$):

$$F_I(b\Delta k, \infty, 0.5, 1) = \frac{4L^2}{b^2} \text{sinc}^2 \left(\frac{\Delta k L}{2} \right)$$

We have seen : tight focus is more efficient, but then negative dispersion required

In region of bound states; index of refraction (with f_i the oscillator strength of transitions)

$$(n-1)_{lines} = \frac{Nr_e}{2\pi} \sum_i \frac{f_i}{\lambda_i^{-2} - \lambda}$$

In the continuum (σ ionization cross section)

$$(n-1)_{continuum} = \frac{N}{2\pi} \int \frac{\sigma}{\bar{v}_i^2 - \bar{v}^2} d\bar{v}_i$$

Cross sections and oscillator strength relate to atomic structure, with C the phase mismatch per atom;

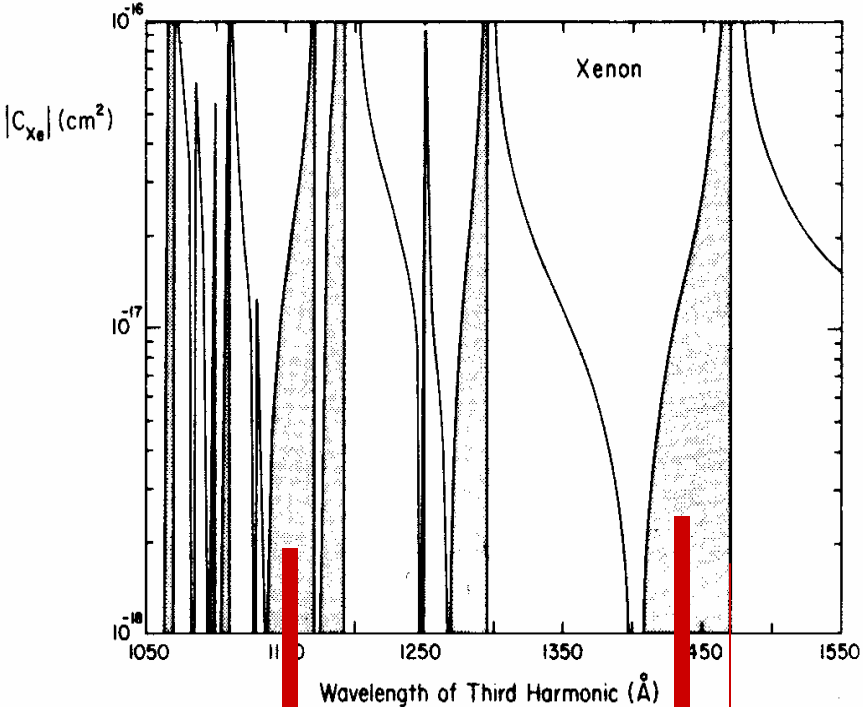
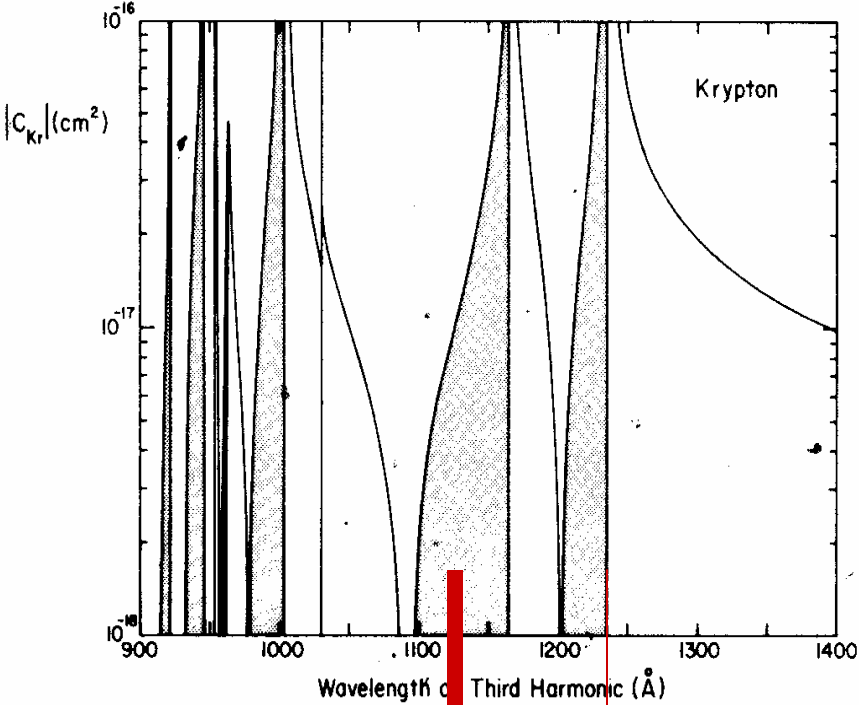
$$\Delta k = CN = \frac{2\pi(n_1 - n_3)}{\lambda}$$



Calculation of regions of positive and negative dispersion

Negative and positive dispersion in the Kr and Xe

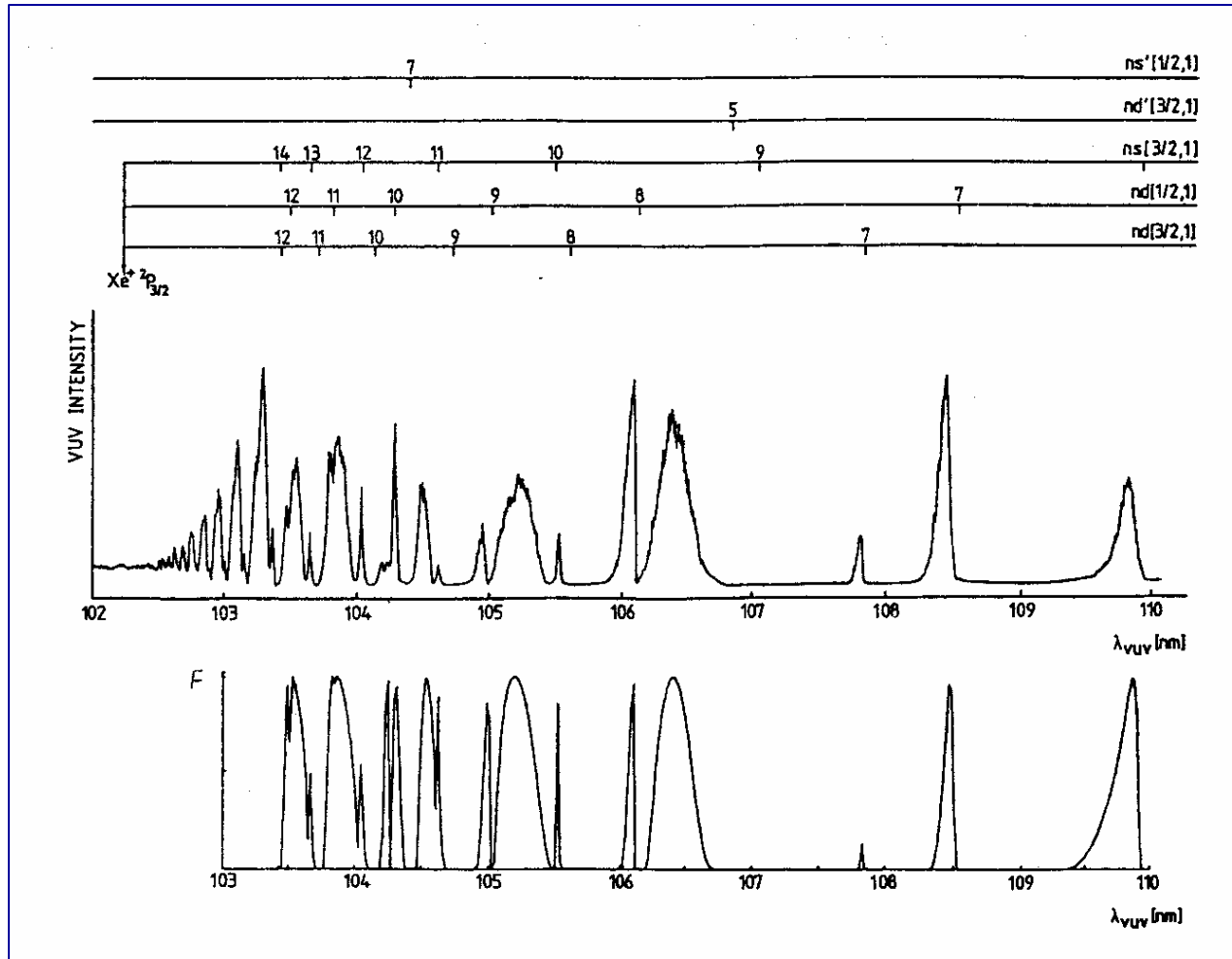
Shaded areas - "anomalous dispersion in the medium"



first resonance line

Regions of efficient THG

THG in Xe; experiment

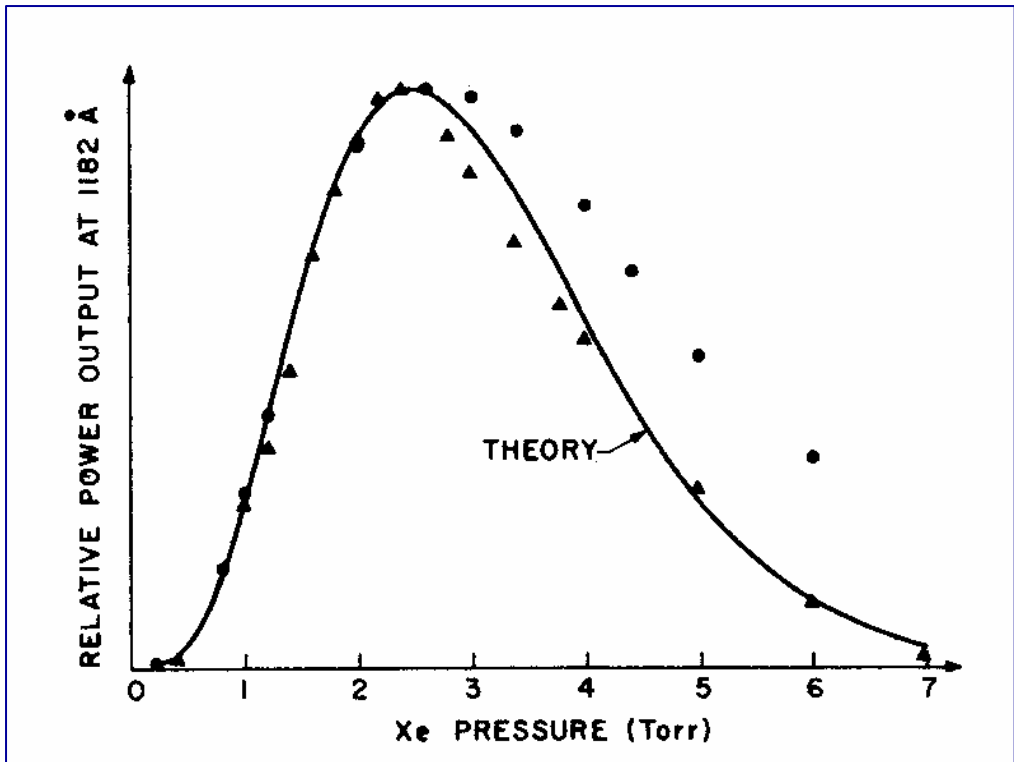


Experiment THG production

Calculation of
Phase-matching integral

Conclusion: 1) theory of phase-matching works
2) THG effective at blue side of ns and nd resonances

Experimental density effect on phase matching in Xe

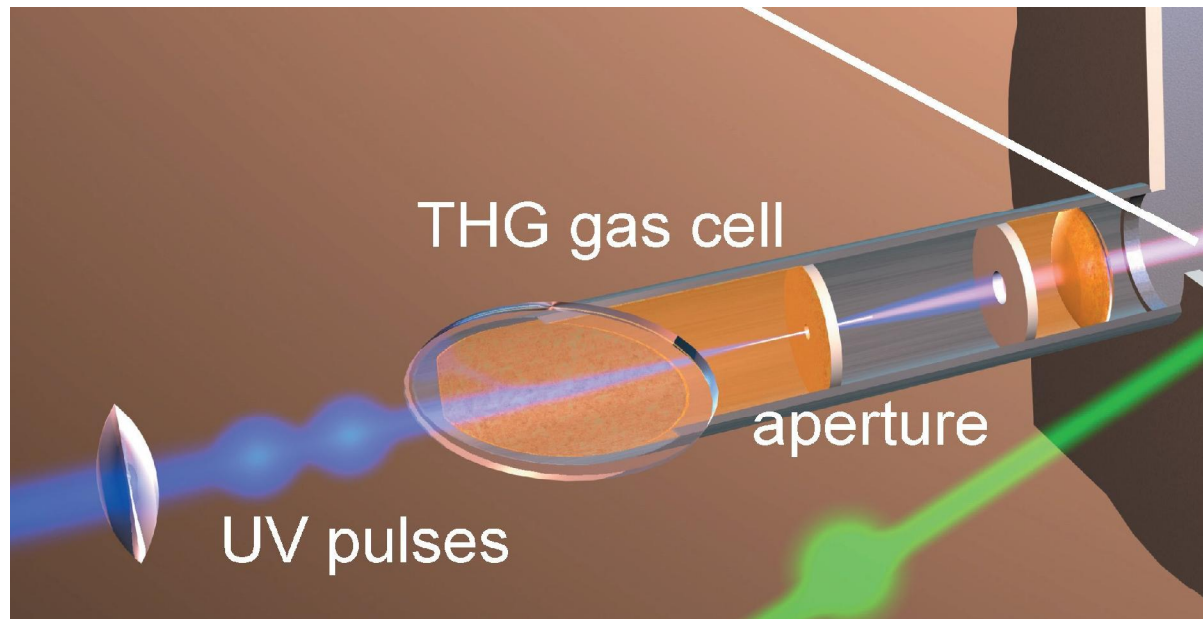


Tight focusing at $\lambda = 118 \text{ nm}$ in Xe
(negative dispersion);
 $b/L = 0.025$
 $f/L = 0.5$ - centre of cell

Effect of G -integral and interplay
between N and Δk .

Defeating the negative dispersion problem

All calculations performed for integral from $-L$ to $+L$.
Cut-off the medium at f ; stop the destructive interference.
Can be done in "forbidden region".
Efficiency remains low; but not zero.



Resonance enhanced VUV production

Non-linear susceptibility:

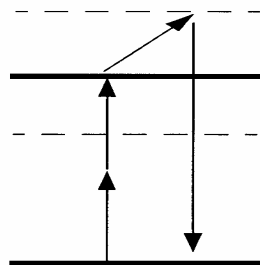
$$\chi^{(3)} \propto \sum_{gijk \text{ terms}} \frac{\langle g|\mathbf{r}|i\rangle\langle i|\mathbf{r}|j\rangle\langle j|\mathbf{r}|k\rangle\langle k|\mathbf{r}|g\rangle}{(\omega_{gi} \pm \omega)(\omega_{gj} \pm 2\omega)(\omega_{gk} \pm 3\omega)}$$

Resonances possible at the

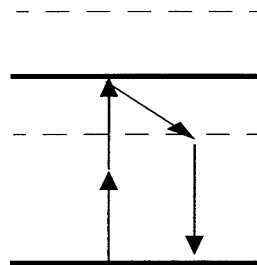
- One photon
- Two-photon
- Three photon levels

Advantage at two-photon-level

$$\chi^{(3)} \propto \sum_{ik \text{ terms}} \frac{\langle g|\mathbf{r}|i\rangle\langle i|\mathbf{r}|J'\rangle\langle J'|\mathbf{r}|k\rangle\langle k|\mathbf{r}|g\rangle}{(\omega_{gi} \pm \omega)(\omega_{gJ'} - 2\omega - i\Gamma)(\omega_{gk} \pm 3\omega)}$$



Process I



Process II

Again level structure of the noble gases is favorable:

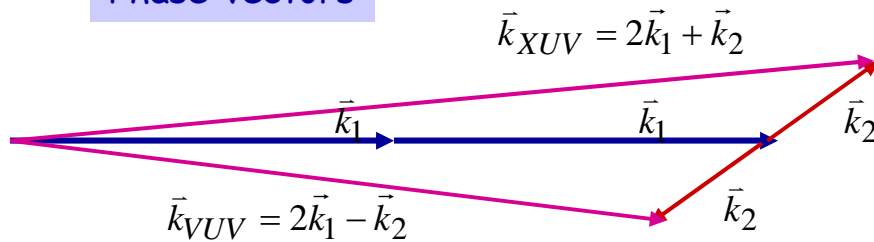
| | Two-photon resonance | excitation energy (cm ⁻¹) | resonance wavelength (nm) | relative efficiency ^a |
|----|-----------------------------|---------------------------------------|---------------------------|----------------------------------|
| Xe | 5p - 6p' [3/2] ₂ | 89162.9 | 224.3 | 40 |
| | [1/2] ₀ | 89860.5 | 222.6 | 187 |
| | 7p [5/2] ₂ | 88352.2 | 226.4 | 4 |
| | [3/2] ₂ | 88687.0 | 225.5 | 9 |
| | [1/2] ₀ | 88842.8 | 225.1 | 26 |
| | 8p [5/2] ₂ | 92221.9 | 216.9 | 9 |
| Kr | [3/2] ₂ | 92371.4 | 216.5 | 5 |
| | [1/2] ₀ | 92555.7 | 216.1 | 119 |
| | 4p - 5p [5/2] ₂ | 92308.2 | 216.7 | 167 |
| | [3/2] ₂ | 93124.1 | 214.8 | 56 |
| | [1/2] ₀ | 94093.7 | 212.6 | 1000 |

^a Fundamental power is 20 kW.

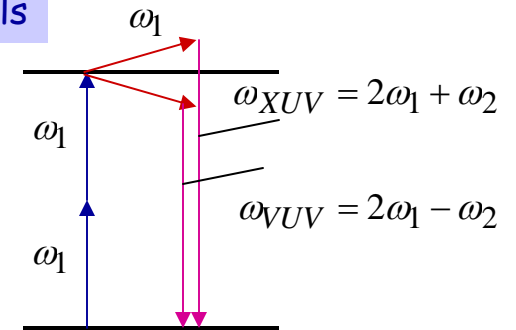
$\lambda = 212.5$ nm resonance in Kr
 "strongest two-photon resonance in nature"

Non-colinear Phase-matching for sum-frequency generation

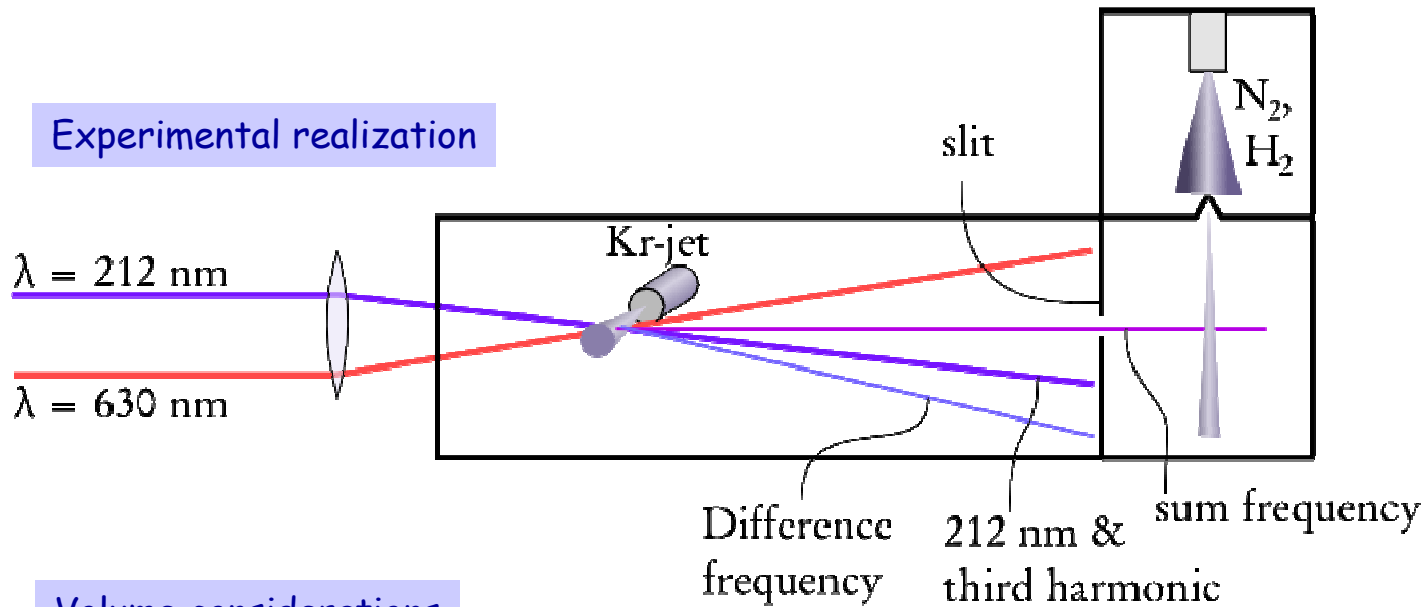
Phase-vectors



Energy levels



Experimental realization



Volume considerations

Polarization properties

Tensor nature of susceptibility

$$\mathbf{P}_\sigma(\omega_r; \omega_i, \omega_j, \omega_k) \propto \chi_{\sigma\alpha\beta\gamma}^{(3)} \mathbf{E}_\alpha^i \mathbf{E}_\beta^j \mathbf{E}_\gamma^k$$

Dependent on matrix dipole moments

$$\chi^{(3)} \propto \sum_{gijk \text{ terms}} \frac{\langle g|\mathbf{r}|i\rangle \langle i|\mathbf{r}|j\rangle \langle j|\mathbf{r}|k\rangle \langle k|\mathbf{r}|g\rangle}{(\omega_{gi} - \omega)(\omega_{gj} - 2\omega)(\omega_{gk} - 3\omega)}$$

Note: a COHERENT sum should be taken
(as in multi-photon transitions)

Parametric and non-parametric processes;
relate to energy exchange

Use atomic physics framework: evaluate
Transition dipole moments with Wigner-Eckhart
theorem:

$$\langle g|\mathbf{r}|i\rangle = \langle J_g M_g | \mathbf{r}_q^{(1)} | J_i M_i \rangle = (-)^{J_i - M_i} \begin{pmatrix} J_i & 1 & J_g \\ -M_i & q & M_g \end{pmatrix} \langle J_g \| \mathbf{r}^{(1)} \| J_i \rangle$$

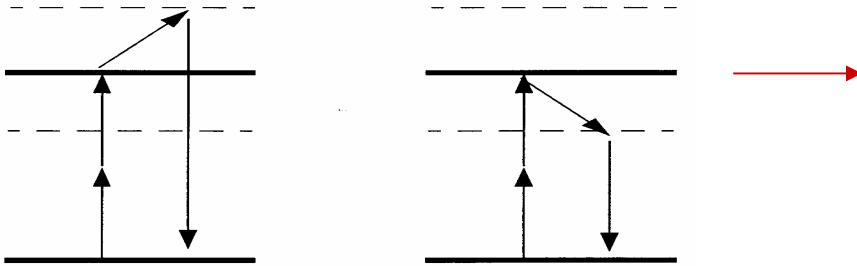
$$\chi^{(3)} \propto \begin{pmatrix} J_i & 1 & J_g \\ -M_i & q_1 & M_g \end{pmatrix} \begin{pmatrix} J_j & 1 & J_i \\ -M_j & q_2 & M_i \end{pmatrix} \begin{pmatrix} J_k & 1 & J_j \\ -M_k & q_3 & M_j \end{pmatrix} \begin{pmatrix} J_g & 1 & J_k \\ -M_g & q_4 & M_k \end{pmatrix}$$

The coherent sum requires $\Delta M=0$ over four-photon cycle;
 $q=0, q=-1, q=1$ projections of dipole moment on angular basis (polarizations)
Evaluate the four-product of Wigner-3j symbols

Results: 1) all polarizations linear is possible $q_1 = q_2 = q_3 = q_4 = 0$

2) THG with circular light is NOT possible: $q_1 = q_2 = q_3 = 1$

Polarization in sum-frequency mixing; quantum levels



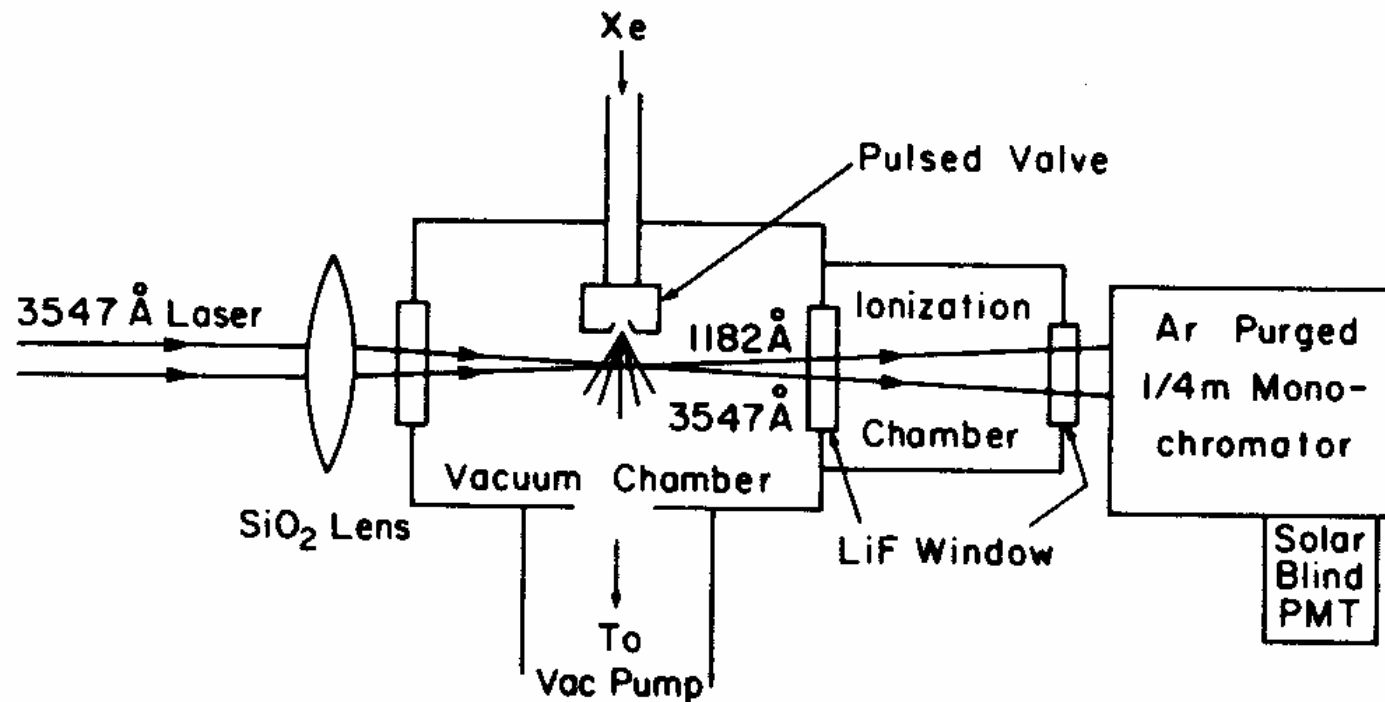
Well defined quantum level;

Real intermediate level

$$J_2 = 0 \text{ or } 2$$

| ω_R | ω_{tun} | ω_{XUV} | $J_2=0$ | $J_2=2$ |
|------------|-----------------------|-----------------------|---------|---------|
| → | → | → | 0.333 | 0.298 |
| → | ↑ | ↑ | 0.333 | -0.149 |
| → | ↻ | → | 0.236 | 0.211 |
| → | ↻ | ↑ | -0.236i | 0.105i |
| ↻ | ↻ | ↻ | 0 | -0.447 |
| ↻ | ↓ | ↻ | 0 | 0.316 |

Pulsed jets and differential pumping - the road to the windowless regime

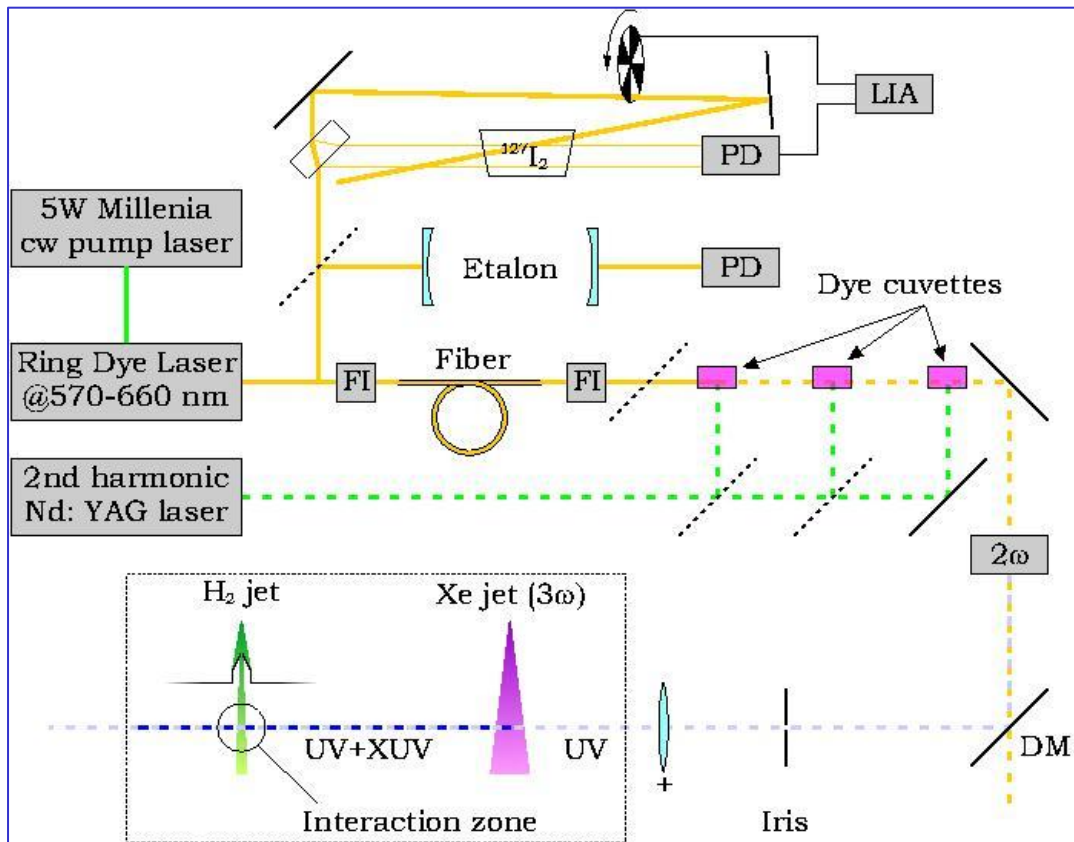


A.H. Kung, Opt. Lett. **8**, 24 (1983).

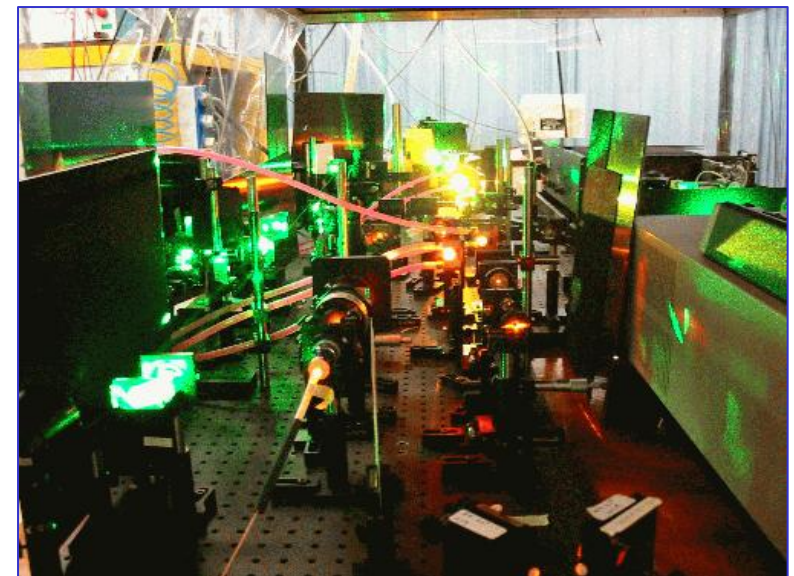
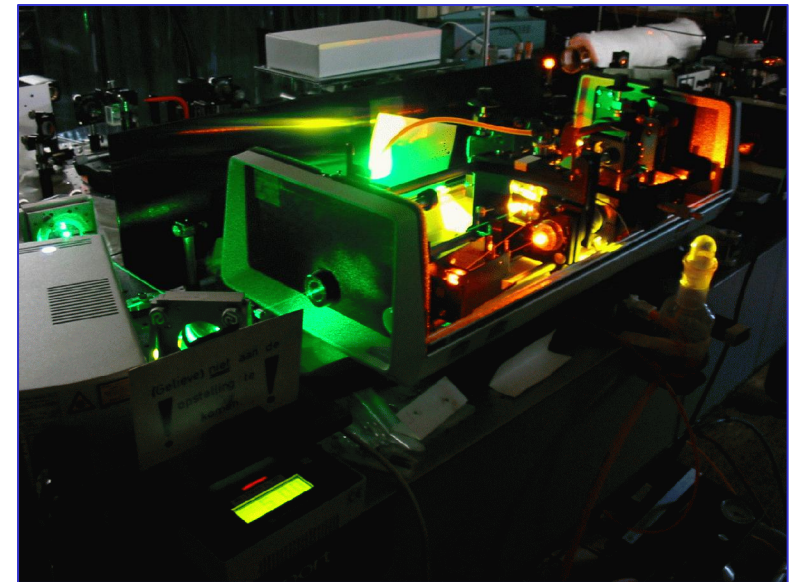
Some considerations

- 1) Bandwidth effects
- 2) Lasers and synchrotrons
- 3) The perturbative regime and the non-perturbative \rightarrow recollision model
- 4) Spectroscopy in VUV and XUV feasible

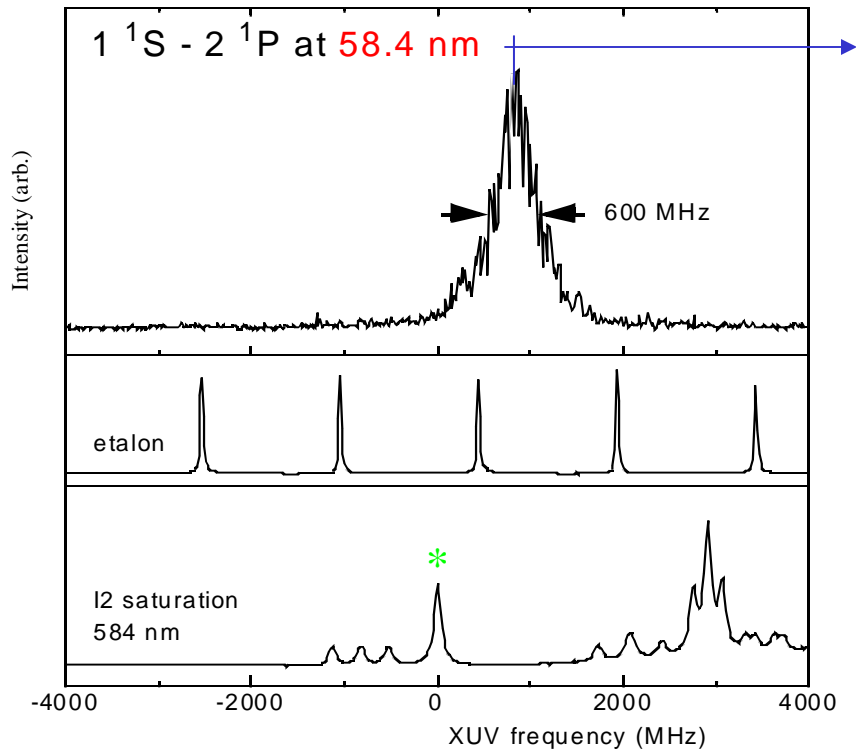
XUV-laser setup with PDA; bandwidth ~250 MHz



$$\lambda = 90 - 110 \text{ nm}$$



Measurement of $1^1S - 2^1P$ resonance line of Helium



* P88(15-1) o component in I₂
at 513049427.1(1.7) MHz

5 130 495 083 (45) MHz

Results on Lamb shift in He ground state

41224 (45) MHz experiment (1997)

41233 (35-100) MHz; Drake (1993)

41223 (42) MHz theory; Korobow/Yelkovsky (2001)

2-electron QED effects in He ($1s^2 \ ^1S_0$)

